

11.4

## Detection of a chaotic signal with noise by quantization over several amplitude levels in the model of a radio engineering chaos generator

© L.V. Kuzmin

Kotelnikov Institute of Radio Engineering and Electronics, Russian Academy of Sciences, Moscow, Russia  
E-mail: lvkuzmin@gmail.com

Received December 22, 2021

Revised April 14, 2022

Accepted April 18, 2022

A method for detecting a continuous chaotic signal with a Gaussian noise by quantizing over four amplitudes and comparing the parameters of the obtained discrete sequence with the parameters of a similar sequence for a non-noisy chaotic signal is proposed. A quantization scheme is developed. It is determined by the structure of the phase space of a dynamic system that generates a chaotic signal. The source of the chaotic signal is a model of a radio engineering generator. The identified chaotic signal has a positive senior Lyapunov exponent and a continuous power spectrum.

**Keywords:** chaotic signals, detection of chaotic signals, non-coherent reception of chaotic signals, quantization of chaotic oscillations.

DOI: 10.21883/TPL.2022.06.53460.19112

Methods for applying chaotic oscillations in solving problems of wireless transmission of information were successfully developed during a few last decades [1,2]. The theoretical and practical interest to the chaotic oscillations is caused by their noise-likeness and related resistance to multipath fading, which is extremely important for wireless transmission of microwave-range information. At present, such oscillations may be practically obtained in almost any microwave frequency band [3]. What is important is that chaotic signals have been included in the set of standards for wireless communications [4].

The downside of noise-likeness of these signals is the complexity of creating such methods for their reception which could provide coherent accumulation of the signal and its detection against the noise. This fact appeared to be a reason for, e.g., developing techniques of chaotic signal differential modulation [5–7], which make unnecessary saving the signal copy in the receiver.

The goal of this work was to create a method for the chaotic signal detection against noise, which is based not upon the signal shape that cannot be reproduced in the receiver but on the properties associated with the phase-space structure of the dynamic system generating the chaotic signal. This approach enables discrete description of the chaotic trajectory based on the laws of the trajectory evolution in the dynamic system phase space and then signal detection against noise by using this description. Here the discretization of the method for representing and utilizing a continuous chaotic signal is similar to symbolic description of the chaotic trajectory [8] but, strictly mathematically, is not identical to it since the symbolic dynamics may be constructed only for a dynamic system with hyperbolic chaos. Examples are known [9–11] of specially synthesized generators possessing this property;

however, the possibility of their practical application is not evident at present.

Here a ring-type radio engineering generator [12] (Fig. 1, *a*) that has been practically tested in the process of creating wired and wireless communication systems [1] is considered as the chaos source.

A task has been set to determine the probability of misdetection of a sum of the chaotic signal  $z(t)$  (with dispersion  $\sigma_z^2$ ) and noise  $n(t)$  (with the unity dispersion) (Fig. 1, *b*)  $T$  in length at the preset signal/noise ratio  $\text{SNR} = 10 \lg(\sigma_z^2/\sigma_n^2)$ .

$$c_S(t_j) = \delta(z(t_j) + \sigma_n n(t_j)) \quad (1)$$

as compared with the pure noise fragment  $T$  in length

$$c_N(t_{j+1}) = \delta \sigma_n n(t_{j+1}), \quad (2)$$

where  $j$  is the fragment number:  $\tau < t_j \leq \tau + T$ ,  $\tau + T < t_{j+1} \leq \tau + 2T$ . Noise  $n(t)$  is formed by filtering a sequence of random Gaussian-distributed samples in such a way that the signal  $n(t)$  frequency band coincides with the chaotic signal  $z(t)$  frequency band (Fig. 1, *c*);  $\tau$  is the moment of the signal (1) fragment origin.

Occurrences of signals (1) and (2) at the detector input are equiprobable.

At the preset SNR value relevant to the preset value of  $\sigma_n$ , dispersion  $c_S(t_j)$  (1) will be normalized to the dispersion of pure chaotic signal  $z(t)$  by multiplying by coefficient  $\delta = \sigma_z / \sqrt{\sigma_z^2 + \sigma_n^2}$  so that signal  $c_S(t_j)$  (1) obtains dispersion  $\sigma_z^2$ . When the signal/noise ratio SNR is varied from minus infinity to plus infinity at constant chaotic signal dispersion  $\sigma_z^2$ ,  $\sigma_n$  varies from  $\sigma_z$  to zero.

Chaotic signal  $z(t)$  is generated by the dynamic system simulating the radio engineering chaos generator (Fig. 1, *a*).

The generator model comprises a piecewise–linear voltage transformation

$$f(V) = |V + E_1| - |V - E_1| + \frac{1}{2}(|V - E_2| - |V + E_2|) \quad (3)$$

and two lower–frequency filters representable by ordinary differential equations

$$R_1 C_1 \dot{V}_{C1} + V_{C1} = m f(V_{C2})$$

and

$$\ddot{V}_{C2} + (R_2/L_2)\dot{V}_{C2} + V_{C2}/(L_2 C_2) = V_{C1}/(L_2 C_2),$$

where  $V_{C1}$ ,  $V_{C2}$  are the voltages at capacitances  $C_1$ ,  $C_2$ , respectively,  $E_1 = V_E/2$ ,  $E_2 = V_E$ . Turning to dimensionless voltage variables  $V_{C1} = V_E x$ ,  $V_{C2} = V_E z$ ,  $E_1 = V_E e_1$ ,  $E_2 = V_E e_2$ ,  $e_1 = 1/2$ ,  $e_2 = 1$  and time variables  $t = t_d \sqrt{L_2 C_2}$ ,  $d/dt = d/(\sqrt{L_2 C_2} dt_d)$  ( $t_d$  is the dimensionless time), introducing coefficients  $\beta = R_1 C_1 / \sqrt{L_2 C_2}$ ,  $\alpha = R_2 \sqrt{C_2/L_2}$ , and excluding variable  $V_{C1}$ , obtain a piecewise–linear third–order equation

$$\beta \ddot{z} + (1 + \beta \alpha) \dot{z} + (\alpha + \beta) z + z = m f(z). \quad (4)$$

The phase space of set (4) in  $z(t)$  (Fig. 1, b) is subdivided by nonlinearity (3) into five regions where function  $f(z)$  retains its linearity

$$\begin{aligned} O_1 : -\infty < z(t) \leq -e_2, \quad f(z(t)) &= 0, \\ O_2 : -e_2 \leq z(t) < -e_1, \quad f(z(t)) &= -z(t) - e_2, \\ O_3 : -e_1 \leq z(t) < e_1, \quad f(z(t)) &= z(t), \\ O_4 : e_1 \leq z(t) < e_2, \quad f(z(t)) &= -z(t) + e_2, \\ O_5 : e_2 \leq z(t) < \infty, \quad f(z(t)) &= 0. \end{aligned} \quad (5)$$

The nonlinearity (3) shape is similar to smooth nonlinearity  $f(z) = z e^{-z^2}$  for which the ring–type generator dynamics has been studied in detail in [12]. It was established that such generators are able to form both periodic and chaotic oscillations in a wide range of parameter values. The advantage of the piecewise–linear transformation (3) is the possibility of its relatively easy realization based on operational amplifiers. Solution of equations (4) demonstrates both the periodic and chaotic behavior. In further calculations we used parameter values  $\beta = 3$ ,  $\alpha = 1/10$ ,  $m = 10$  (the step of the equation set (4) Runge–Kutta integration was  $\Delta T = 0.05$ ) corresponding to the chaotic oscillation mode with a continuous power spectrum (Fig. 1, c) and positive senior Lyapunov exponent.

Eigenvalues for the third–order equation set (4) may be explicitly found in regions (5). Eigenvalues in region  $O_3$  look as follows:

$$\begin{aligned} \lambda_1^{(3)} &= Q - \frac{2621}{8100Q} - \frac{13}{90}, \\ \lambda_{2,3}^{(3)} &= -\frac{1}{2} \left( \lambda_1^{(3)} + \frac{13}{90} \right) \pm \frac{\sqrt{3} \left( \frac{2621}{8100Q} + Q \right) i}{2}, \end{aligned}$$

where

$$Q = \left( \frac{m}{6} + \sqrt{\left( \frac{m}{6} - \frac{17323}{182250} \right)^2 + \frac{18005329061}{531441000000} - \frac{17323}{182250}} \right)^{1/3}.$$

Eigenvalues in regions  $O_2$  and  $O_4$  are

$$\begin{aligned} \lambda_1^{(2,4)} &= R - \frac{2621}{8100R} - \frac{13}{90}, \\ \lambda_{2,3}^{(2,4)} &= -\frac{1}{2} \left( \lambda_1^{(2,4)} + \frac{13}{90} \right) \pm \frac{\sqrt{3} \left( \frac{2621}{8100Q} + R \right) i}{2}, \end{aligned}$$

where  $R = (Q^3 - \frac{m}{3})^{1/3}$ . Real parts of all the specified eigenvalues are above zero, i.e. equilibrium states in regions  $O_2$ ,  $O_3$ ,  $O_4$  are unstable, and the phase trajectory leaves their vicinity during its evolution. In regions  $O_1$ ,  $O_5$ , real parts of eigenvalues  $\lambda_1^{(1,5)} = -1/3$ ,  $\lambda_{2,3}^{(1,5)} = -1/20 \pm \sqrt{399}i/20$  are negative; the equilibrium position coincides with the coordinate origin, hence, the trajectory from regions  $O_1$ ,  $O_5$  evolves into region  $O_2$  or  $O_4$ , and the equation set (4) oscillations as a whole are always limited.

During its evolution, the  $z(t)$  trajectory crosses the boundaries of regions  $z_1^{(\pm)} = \pm e_1$  and  $z_2^{(\pm)} = \pm e_2$  which define four amplitude levels comparison with which allows revealing to what phase–space region (5) the current  $z(t)$  value belongs. Let us introduce symbolic designation  $Z_i^{(k)}$  indicating the belongingness of the  $z(t)$  trajectory sections to phase–space regions (5):

$$Z_i^{(k)} = \begin{cases} 1, & k = 1, & z(t) \in O_1, \\ 2, & k = 2, & z(t) \in O_2, \\ 3, & k = 3, & z(t) \in O_3, \\ 4, & k = 4, & z(t) \in O_4, \\ 5, & k = 5, & z(t) \in O_5. \end{cases} \quad (6)$$

Here index  $i$  is the symbol number in the sequence generated by signal  $z(t)$  as per (6), while  $k$  is the symbol type. After transformation (6) of continuous signal  $z(t)$ , obtain a discrete representation of the signal in the form of a sequence of symbols

$$\dots Z_{i-1}^{(k_{i-1})}, Z_i^{(k_i)}, Z_{i+1}^{(k_{i+1})}, \dots, Z_{i+N-1}^{(k_{i+N-1})}, Z_{i+N}^{(k_{i+N})} \dots \quad (7)$$

For instance, sequence „5432121234321234345“ corresponds to fragment (1) (Fig. 1, b) in section [0,25], while sequence „32343“ corresponds to section [125,150].

The detection method presented here is based on monitoring the sequence of regions (5) interchange and comparing the frequencies of occurrence of single, double, triple, and so on combinations of symbols (6) calculated for pure chaotic signal  $z(t)$  with the frequency of occurrence of symbol groups generated by signals (1) and (2).

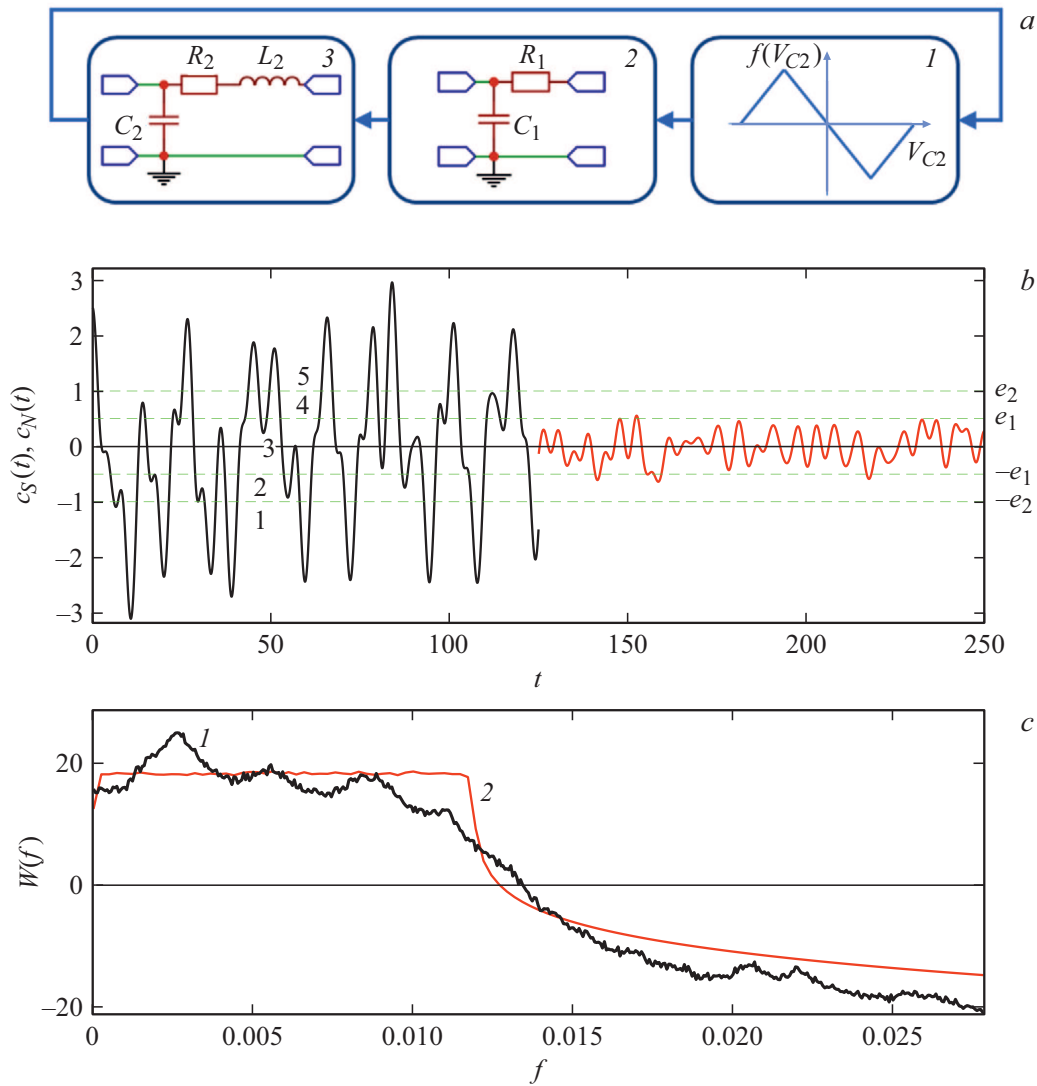


**Figure 1.** *a*— the chaos generator structure: 1 nonlinear transformation, 2, 3 filters of the first–order and second–order lower frequencies, respectively; *b*— examples of realizing fragments of signals  $c_S(t_j)$  (1) (interval  $[0,125]$ ) and  $c_N(t_{j+1})$  (2) (interval  $[125,250]$ ) at the signal/noise ratio SNR = 12 dB; the dashed lines indicate subdivision (5); *c*— power spectrum  $W(f)$  of the non–noisy chaotic signal  $z(t)$  (curve 1) and noise  $n(t)$  (curve 2).

Designate as  $S_j(L) = Z_i^{(k_0)}, Z_{i+1}^{(k_1)}, \dots, Z_{i+L-1}^{(k_{L-1})}$  the  $j$ -th group (combination) consisting of  $L$  symbols formed from sequence (7): if  $L = 1$ , they are single symbols, if  $L = 2$ , they are pair combinations, etc. Group  $(j + 1)$  is formed by shifting by one symbol, i.e.  $S_{j+1}(L) = Z_{i+1}^{(k_1)}, Z_{i+2}^{(k_2)}, \dots, Z_{i+L}^{(k_L)}$ . The total number of possible groups is  $Q(L) = 5^L$  of any and all possible rearrangements of  $L$  symbols. Let  $p_C^{(q)}(S_q(L))$  (where  $q = 1, \dots, Q(L)$ ) be the frequencies of occurrence of groups  $S_q(L)$  for the pure chaotic signal and  $p_N^{(q)}(S_q(L))$  — those for pure noise with the band and dispersion equal to the band and dispersion of the chaotic signal. The sums of the symbol group occurrence frequencies are normalized to unity:  $\sum_{q=1}^{q=Q(L)} p_C^{(q)} = \sum_{q=1}^{q=Q(L)} p_N^{(q)} = 1$ .

Modeling shows that not all  $5^L$  possible symbol groups come into effect, i.e., number  $N_C(L)$  of permissible combinations  $L$  in length (Fig. 2) for the chaotic signal does not exceed  $N_N(L)$  for the noise, and their frequencies are different:  $N_C(L) \leq N_N(L)$ ,  $p_C^{(q)}(S_q(L)) \neq p_N^{(q)}(S_q(L))$ ,  $q = 1, \dots, Q(L)$ . This property is the basis of the signals (1) and (2) classification method to realize which the following norm expressed via the symbol group occurrence frequencies (coinciding for both signals) was introduced:

$$D^{(L)}(p_S) = \sum_{q=1}^{\max(N_S, N_C)} |p_C^{(q)}(S_q(L)) - p_S^{(q)}(S_q(L))|, \quad (8)$$

where  $N_C$  is the number of different  $S_q(L)$  groups detectable in the pure chaotic signal, while  $N_S$  is that in the signal with which it is compared (signal under classification);  $p_S^{(q)}$  are

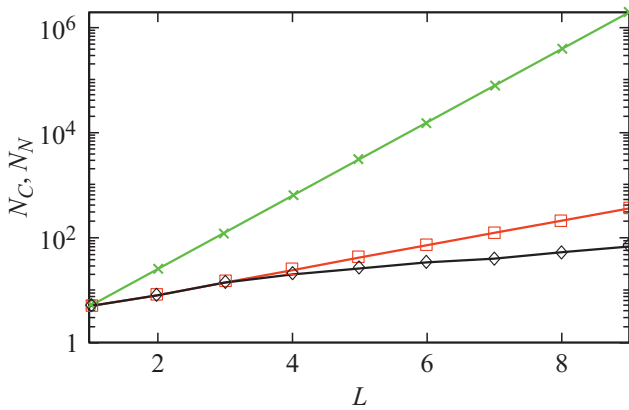


**Figure 2.** Number  $N_C$  of permissible groups of symbols  $S_q(L)$  for the chaotic signal (diamonds), number  $N_N$  for the noise in the chaotic signal band (squares), and total possible number of groups  $L$  in length (crosses).

the frequencies of the symbol groups occurrence in the signal under classification. If the symbol combination is absent in one of the signals, its occurrence frequency is assumed to be zero for this signal. For signal (1)  $p_S^{(q)} = p_{C_S}^{(q)}$ , for signal (2)  $p_S^{(q)} = p_{C_N}^{(q)}$ , where  $p_{C_S}^{(q)}$  and  $p_{C_N}^{(q)}$  are the symbols  $S_q(L)$  occurrence frequencies for signals (1) and (2), respectively.

Let norm  $D^{(L)}(p_{C_S})$  be defined according to (8) for pair „pure chaos–signal (1)“ and norm  $D^{(L)}(p_{C_N})$  be defined for pair „pure chaos–signal (2)“. Based on  $\rho_{C_S}(D^{(L)}(p_{C_S}))$  and  $\rho_{C_N}(D^{(L)}(p_{C_N}))$ , determine for the preset SNR the densities of the conditional probabilities of receiving signal (1) and signal (2), respectively. If  $\text{SNR} \rightarrow +\infty$ , then  $\sigma_n \rightarrow 0$  (in view of the signal and noise power normalization), and mean values behave as  $\langle D^{(L)}(p_{C_S}) \rangle \rightarrow 0$ ,  $\langle D^{(L)}(p_{C_N}) \rangle \rightarrow 1$ .

The test statistics for classifying an unknown signal of type (1) or (2) with symbol group occurrence frequencies  $p_S^{(q)}$  is defined as  $D_T^{(L)} = D^{(L)}(p_S) - \gamma_0$ . The signal will be classified as (1) if  $D_T^{(L)} < 0$  and (2) if  $D_T^{(L)} > 0$ .

The threshold value  $\gamma_0$  that is to be calculated *a priori* for the preset SNR will be found by minimizing sum  $\int_{\gamma_0}^{+\infty} \rho_{C_S} dD^{(L)} + \int_{-\infty}^{\gamma_0} \rho_{C_N} dD^{(L)}$  of frequencies of false–negative and false–positive errors.

Examples of densities  $\rho_{C_S}$  and  $\rho_{C_N}$  are shown in Fig. 3, *a* (SNR = 0 dB,  $L = 1$ ). The probability densities were calculated for the signal/noise ratio SNR ranging from  $-8$  to 3 dB with the step of 0.5 dB. For each SNR value, threshold  $\gamma_0$  was determined *a priori*, and the sum of empiric frequencies of classifying „signal (1) as signal (2)“ and „signal (2) as signal (1)“ was calculated; this sum is presented in Fig. 3, *b* as a function of SNR.

The method described was used to find an answer to the question of great practical importance: whether it is

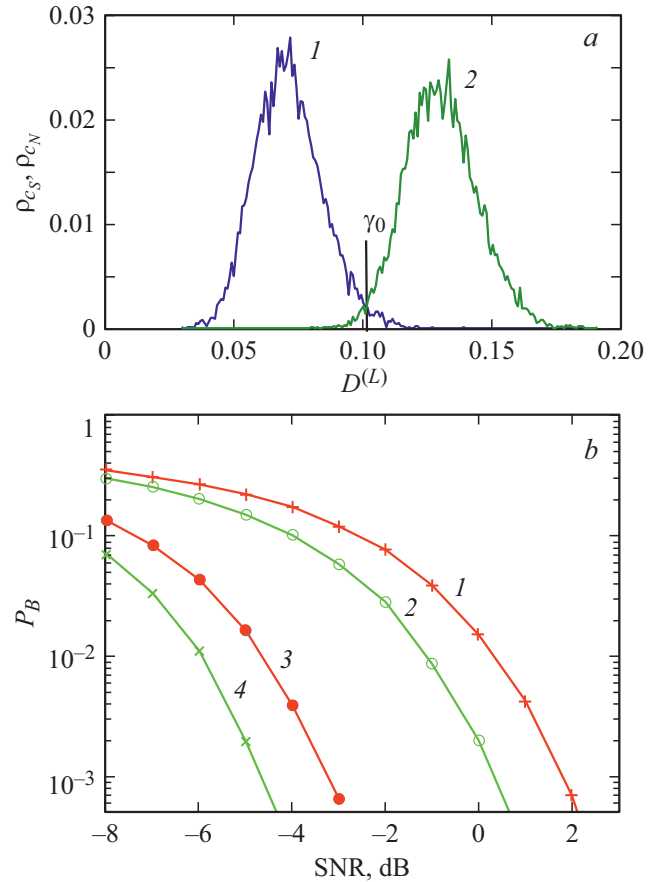


**Figure 3.** Conditional probability densities  $\rho_{C_S}(D^{(L)}(p_{C_S}))$  (curve 1) and  $\rho_{C_N}(D^{(L)}(p_{C_N}))$  (curve 2) at SNR = 0 dB (*a*), and sum  $P_B$  of empiric frequencies of the „signal (1) as signal (2)“ and „signal (2) as signal (1)“ classifications at the signal/noise ratio SNR ranging from  $-8$  to 3 dB for different pulse lengths  $T$  and different symbol numbers  $L$  in the group: 1 –  $T = 1032$ ,  $L = 1$ ; 2 –  $T = 1032$ ,  $L = 2$ ; 3 –  $T = 8256$ ,  $L = 1$ ; 4 –  $T = 8256$ ,  $L = 2$ . The calculation was performed for  $10^4$  classified examples.

possible using the given detection system to decrease the misdetection frequency by increasing: (i) signals (1) and (2) lengths; (ii) symbol number  $L$  in the group for detecting (1) as compared with (2).

A positive answer was obtained for this question: with increasing length  $T$  of signals (1) and (2), the accumulation effect takes place, i. e., the misdetection frequency decreases (Fig. 3, *b*). For instance, the eightfold increase in signal (1) and (2) length  $T$  at the error frequency of  $10^{-3}$  allows worsening the signal/noise ratio by 5 dB. The increase in the symbol number  $L$  in the group from one to two also reduces the error probability by 2 dB.

Thus, this paper presents a method for detecting a chaotic signal with noise, which enables distinguishing the chaotic signal from noise over four levels of amplitude quantization, which is practically attractive. The method does not require knowing the signal phase or using timing.

## Financial support

The study was supported by the Russian Fundamental Research Foundation (grant № 20-02-00877 A).

## Conflict of interests

The author declares that he has no conflict of interests.

## References

- [1] A.S. Dmitriev, A.I. Panas, *Dinamichesky khaos: novye nositeli informatsii dlya sistem svyazi* (Fizmatlit, M., 2002). (in Russian)
- [2] G. Kaddoum, *IEEE Access*, **4**, 2621 (2016). DOI: 10.1109/ACCESS.2016.2572730
- [3] A.S. Dmitriev, E.V. Efremova, A.I. Panas, N.A. Maksimov, *Generatsiya khaosa* (Tekhnosfera, M., 2012). (in Russian)
- [4] V. Niemelä, J. Haapola, M. Hämäläinen, J. Iinatti, *IEEE Commun. Surv. Tutorials*, **19** (2), 874 (2017). DOI: 10.1109/COMST.2016.2634593
- [5] A.S. Dmitriev, T.I. Mokhseni, K.M. Sierra-Teran, *J. Commun. Technol. Electron.*, **63**(10), 1183 (2018). DOI: 10.1134/S1064226918100078.
- [6] A.S. Dmitriev, T.I. Mokhseni, C.M. Sierra-Teran, *Tech. Phys. Lett.*, **46** (7), 669 (2020). DOI: 10.1134/S106378502007007X.
- [7] G. Kolumban, M. Kennedy, *IEEE Trans. Circ. Syst. I*, **44** (10), 927 (1997). DOI: 10.1109/81.633882
- [8] J. Schweizer, T. Schimming, *IEEE Trans. Circ. Syst. I*, **48** (11), 1283 (2001). DOI: 10.1109/81.964417
- [9] S.P. Kuznetsov, *Phys. Rev. Lett.*, **95** (14), 144101 (2005). DOI: 10.1103/PhysRevLett.95.144101
- [10] N.J. Corron, J.N. Blakely, M.T. Stahl, *Chaos*, **20** (2), 023123 (2010). DOI: 10.1063/1.3432557
- [11] C. Bai, H. Ren, C. Grebogi, *IEEE Access*, **7**, 25274 (2019). DOI: 10.1109/ACCESS.2019.2900729
- [12] A.S. Dmitriev, A.I. Panas, S.O. Starkov, *Int. J. Bifur. Chaos*, **6** (5), 851 (1996). DOI: 10.1142/S0218127496000473